2-15-1996

Rapidity Gaps Between Jets in Photoproduction at HERA

M. Derrick
Argonne National Laboratory

D. Krakauer
Argonne National Laboratory

S. Magill
Argonne National Laboratory

D. Mikunas
Argonne National Laboratory

B. Musgrave
Argonne National Laboratory

See next page for additional authors

DESY 95-194
October 1995

Rapidity Gaps between Jets in Photoproduction at HERA

ZEUS Collaboration

Abstract

Photoproduction events which have two or more jets have been studied in the $W_{\gamma p}$ range 135 GeV $< W_{\gamma p} <$ 280 GeV with the ZEUS detector at HERA. A class of events is observed with little hadronic activity between the jets. The jets are separated by pseudorapidity intervals ($\Delta\eta$) of up to four units and have transverse energies greater than 6 GeV. A gap is defined as the absence between the jets of particles with transverse energy greater than 300 MeV. The fraction of events containing a gap is measured as a function of $\Delta\eta$. It decreases exponentially as expected for processes in which colour is exchanged between the jets, up to a value of $\Delta\eta \sim 3$, then reaches a constant value of about 0.1. The excess above the exponential fall-off can be interpreted as evidence for hard diffractive scattering via a strongly interacting colour singlet object.

The ZEUS Collaboration

M. Derrick, D. Krakauer, S. Magill, D. Mikunas, B. Musgrave, J. Repond, R. Stanek, R.L. Talaga, H. Zhang
Argonne National Laboratory, Argonne, IL, USA [p]

G. Bari, M. Basile, L. Bellagamba, D. Boscherini, A. Bruni, G. Bruni, P. Bruni, G. Cara Romeo, G. Castellini[1], M. Chiarini, L. Cifarelli[2], F. Cindolo, A. Contin, M. Corradi, I. Gialas[3], P. Giusti, G. Iacobucci, G. Laurenti, G. Levi, A. Margotti, T. Massam, R. Nania, C. Nemoz, F. Palmonari, A. Polini, G. Sartorelli, R. Timellini, Y. Zamora Garcia[4], A. Zichichi
University and INFN Bologna, Bologna, Italy [f]

A. Bornheim, J. Crittenden, K. Desch, B. Diekmann[5], T. Doeker, M. Eckert, L. Feld, A. Frey, M. Geerts, M. Grothe, H. Hartmann, K. Heinloth, L. Heinz, E. Hilger, H.-P. Jakob, U.F. Katz, S. Mengel, J. Mollen[6], E. Paul, M. Pfeiffer, Ch. Rembser, D. Schramm, J. Stamm, R. Wedemeyer
Physikalisches Institut der Universität Bonn, Bonn, Germany [c]

S. Campbell-Robson, A. Cassidy, W.N. Cottingham, N. Dyce, B. Foster, S. George, M.E. Hayes, G.P. Heath, H.F. Heath, C.J.S. Morgado, J.A. O'Mara, D. Piccioni, D.G. Roff, R.J. Tapper, R. Yoshida
H.H. Wills Physics Laboratory, University of Bristol, Bristol, U.K. [o]

R.R. Rau
Brookhaven National Laboratory, Upton, L.I., USA [p]

M. Arneodo[7], R. Ayad, M. Capua, A. Garfagnini, L. Iannotti, M. Schioppa, G. Susinno
Calabria University, Physics Dept.and INFN, Cosenza, Italy [f]

A. Bernstein, A. Caldwell[8], N. Cartiglia, J.A. Parsons, S. Ritz[9], F. Sciulli, P.B. Straub, L. Wai, S. Yang, Q. Zhu
Columbia University, Nevis Labs., Irvington on Hudson, N.Y., USA [q]

P. Borzemski, J. Chwastowski, A. Eskreys, K. Piotrzkowski, M. Zachara, L. Zawiejski
Inst. of Nuclear Physics, Cracow, Poland [j]

L. Adamczyk, B. Bednarek, K. Jeleń, D. Kisielewska, T. Kowalski, M. Przybycień, E. Rulikowska-Zarębska, L. Suszycki, J. Zając
Faculty of Physics and Nuclear Techniques, Academy of Mining and Metallurgy, Cracow, Poland [j]

A. Kotański
Jagellonian Univ., Dept. of Physics, Cracow, Poland [k]

L.A.T. Bauerdick, U. Behrens, H. Beier, J.K. Bienlein, C. Coldewey, O. Deppe, K. Desler, G. Drews, M. Flasiński[10], D.J. Gilkinson, C. Glasman, P. Göttlicher, J. Große-Knetter, B. Gutjahr[11], T. Haas, W. Hain, D. Hasell, H. Heßling, Y. Iga, K.F. Johnson[12], P. Joos, M. Kasemann, R. Klanner, W. Koch, L. Köpke[13], U. Kötz, H. Kowalski, J. Labs, A. Ladage, B. Löhr, M. Löwe, D. Lüke, J. Mainusch[14], O. Mańczak, T. Monteiro[15], J.S.T. Ng, S. Nickel[16], D. Notz, K. Ohrenberg, M. Roco, M. Rohde, J. Roldán, U. Schneekloth, W. Schulz, F. Selonke, E. Stiliaris[17], B. Surrow, T. Voß, D. Westphal, G. Wolf, C. Youngman, W. Zeuner, J.F. Zhou[18]
Deutsches Elektronen-Synchrotron DESY, Hamburg, Germany

H.J. Grabosch, A. Kharchilava[19], A. Leich, S.M. Mari[3], M.C.K. Mattingly[20], A. Meyer, S. Schlenstedt, N. Wulff
DESY-Zeuthen, Inst. für Hochenergiephysik, Zeuthen, Germany

G. Barbagli, E. Gallo, P. Pelfer
University and INFN, Florence, Italy [f]

G. Anzivino, G. Maccarrone, S. De Pasquale, L. Votano
INFN, Laboratori Nazionali di Frascati, Frascati, Italy [f]

A. Bamberger, S. Eisenhardt, A. Freidhof, S. Söldner-Rembold[21], J. Schroeder[22], T. Trefzger
Fakultät für Physik der Universität Freiburg i.Br., Freiburg i.Br., Germany [c]

N.H. Brook, P.J. Bussey, A.T. Doyle, D.H. Saxon, M.L. Utley, A.S. Wilson
Dept. of Physics and Astronomy, University of Glasgow, Glasgow, U.K. [o]

A. Dannemann, U. Holm, D. Horstmann, T. Neumann, R. Sinkus, K. Wick
Hamburg University, I. Institute of Exp. Physics, Hamburg, Germany [c]

E. Badura[23], B.D. Burow[24], L. Hagge[14], E. Lohrmann, J. Milewski, M. Nakahata[25], N. Pavel, G. Poelz, W. Schott, F. Zetsche
Hamburg University, II. Institute of Exp. Physics, Hamburg, Germany [c]

T.C. Bacon, N. Bruemmer, I. Butterworth, V.L. Harris, B.Y.H. Hung, K.R. Long, D.B. Miller, P.P.O. Morawitz, A. Prinias, J.K. Sedgbeer, A.F. Whitfield
Imperial College London, High Energy Nuclear Physics Group, London, U.K. [o]

U. Mallik, E. McCliment, M.Z. Wang, S.M. Wang, J.T. Wu
University of Iowa, Physics and Astronomy Dept., Iowa City, USA [p]

P. Cloth, D. Filges
Forschungszentrum Jülich, Institut für Kernphysik, Jülich, Germany

S.H. An, S.M. Hong, S.W. Nam, S.K. Park, M.H. Suh, S.H. Yon
Korea University, Seoul, Korea [h]

R. Imlay, S. Kartik, H.-J. Kim, R.R. McNeil, W. Metcalf, V.K. Nadendla
Louisiana State University, Dept. of Physics and Astronomy, Baton Rouge, LA, USA [p]

F. Barreiro[26], G. Cases, J.P. Fernandez, R. Graciani, J.M. Hernández, L. Hervás[26], L. Labarga[26], M. Martinez, J. del Peso, J. Puga, J. Terron, J.F. de Trocóniz
Univer. Autónoma Madrid, Depto de Física Teóríca, Madrid, Spain [n]

G.R. Smith
University of Manitoba, Dept. of Physics, Winnipeg, Manitoba, Canada [a]

F. Corriveau, D.S. Hanna, J. Hartmann, L.W. Hung, J.N. Lim, C.G. Matthews, P.M. Patel, L.E. Sinclair, D.G. Stairs, M. St.Laurent, R. Ullmann, G. Zacek
McGill University, Dept. of Physics, Montréal, Québec, Canada [a, b]

V. Bashkirov, B.A. Dolgoshein, A. Stifutkin
Moscow Engineering Physics Institute, Moscow, Russia [l]

G.L. Bashindzhagyan[27], P.F. Ermolov, L.K. Gladilin, Yu.A. Golubkov, V.D. Kobrin, I.A. Korzhavina, V.A. Kuzmin, O.Yu. Lukina, A.S. Proskuryakov, A.A. Savin, L.M. Shcheglova, A.N. Solomin, N.P. Zotov
Moscow State University, Institute of Nuclear Physics, Moscow, Russia [m]

M. Botje, F. Chlebana, A. Dake, J. Engelen, M. de Kamps, P. Kooijman, A. Kruse, H. Tiecke, W. Verkerke, M. Vreeswijk, L. Wiggers, E. de Wolf, R. van Woudenberg[28]
NIKHEF and University of Amsterdam, Netherlands [i]

D. Acosta, B. Bylsma, L.S. Durkin, J. Gilmore, K. Honscheid, C. Li, T.Y. Ling, K.W. McLean[29], P. Nylander, I.H. Park, T.A. Romanowski[30], R. Seidlein[31]
Ohio State University, Physics Department, Columbus, Ohio, USA [p]

D.S. Bailey, A. Byrne[32], R.J. Cashmore, A.M. Cooper-Sarkar, R.C.E. Devenish, N. Harnew, M. Lancaster, L. Lindemann[3], J.D. McFall, C. Nath, V.A. Noyes, A. Quadt, J.R. Tickner, H. Uijterwaal, R. Walczak, D.S. Waters, F.F. Wilson, T. Yip
Department of Physics, University of Oxford, Oxford, U.K. [o]

G. Abbiendi, A. Bertolin, R. Brugnera, R. Carlin, F. Dal Corso, M. De Giorgi, U. Dosselli, S. Limentani, M. Morandin, M. Posocco, L. Stanco, R. Stroili, C. Voci
Dipartimento di Fisica dell' Universita and INFN, Padova, Italy [f]

J. Bulmahn, J.M. Butterworth, R.G. Feild, B.Y. Oh, J.R. Okrasinski[33], J.J. Whitmore
Pennsylvania State University, Dept. of Physics, University Park, PA, USA [q]

G. D'Agostini, G. Marini, A. Nigro, E. Tassi
Dipartimento di Fisica, Univ. 'La Sapienza' and INFN, Rome, Italy [f]

J.C. Hart, N.A. McCubbin, K. Prytz, T.P. Shah, T.L. Short
Rutherford Appleton Laboratory, Chilton, Didcot, Oxon, U.K. [o]

E. Barberis, T. Dubbs, C. Heusch, M. Van Hook, W. Lockman, J.T. Rahn, H.F.-W. Sadrozinski, A. Seiden, D.C. Williams
University of California, Santa Cruz, CA, USA [p]

J. Biltzinger, R.J. Seifert, O. Schwarzer, A.H. Walenta, G. Zech
Fachbereich Physik der Universität-Gesamthochschule Siegen, Germany [c]

H. Abramowicz, G. Briskin, S. Dagan[34], C. Händel-Pikielny, A. Levy[27]
School of Physics,Tel-Aviv University, Tel Aviv, Israel [e]

J.I. Fleck, T. Hasegawa, M. Hazumi, T. Ishii, M. Kuze, S. Mine, Y. Nagasawa, M. Nakao, I. Suzuki, K. Tokushuku, S. Yamada, Y. Yamazaki
Institute for Nuclear Study, University of Tokyo, Tokyo, Japan [g]

M. Chiba, R. Hamatsu, T. Hirose, K. Homma, S. Kitamura, Y. Nakamitsu, K. Yamauchi
Tokyo Metropolitan University, Dept. of Physics, Tokyo, Japan [g]

R. Cirio, M. Costa, M.I. Ferrero, L. Lamberti, S. Maselli, C. Peroni, R. Sacchi, A. Solano, A. Staiano
Universita di Torino, Dipartimento di Fisica Sperimentale and INFN, Torino, Italy [f]

M. Dardo
II Faculty of Sciences, Torino University and INFN - Alessandria, Italy [f]

D.C. Bailey, D. Bandyopadhyay, F. Benard, M. Brkic, D.M. Gingrich[35], G.F. Hartner, K.K. Joo, G.M. Levman, J.F. Martin, R.S. Orr, S. Polenz, C.R. Sampson, R.J. Teuscher
University of Toronto, Dept. of Physics, Toronto, Ont., Canada [a]

C.D. Catterall, T.W. Jones, P.B. Kaziewicz, J.B. Lane, R.L. Saunders, J. Shulman
University College London, Physics and Astronomy Dept., London, U.K. [o]

K. Blankenship, B. Lu, L.W. Mo
Virginia Polytechnic Inst. and State University, Physics Dept., Blacksburg, VA, USA [q]

W. Bogusz, K. Charchuła, J. Ciborowski, J. Gajewski, G. Grzelak[36], M. Kasprzak, M. Krzyżanowski, K. Muchorowski[37], R.J. Nowak, J.M. Pawlak, T. Tymieniecka, A.K. Wróblewski, J.A. Zakrzewski, A.F. Żarnecki
Warsaw University, Institute of Experimental Physics, Warsaw, Poland [j]

M. Adamus
Institute for Nuclear Studies, Warsaw, Poland [j]

Y. Eisenberg[34], U. Karshon[34], D. Revel[34], D. Zer-Zion
Weizmann Institute, Particle Physics Dept., Rehovot, Israel [d]

I. Ali, W.F. Badgett, B. Behrens[38], S. Dasu, C. Fordham, C. Foudas, A. Goussiou[39], R.J. Loveless, D.D. Reeder, S. Silverstein, W.H. Smith, A. Vaiciulis, M. Wodarczyk
University of Wisconsin, Dept. of Physics, Madison, WI, USA [p]

T. Tsurugai
Meiji Gakuin University, Faculty of General Education, Yokohama, Japan

S. Bhadra, M.L. Cardy, C.-P. Fagerstroem, W.R. Frisken, K.M. Furutani, M. Khakzad, W.N. Murray, W.B. Schmidke
York University, Dept. of Physics, North York, Ont., Canada [a]

[1] also at IROE Florence, Italy
[2] now at Univ. of Salerno and INFN Napoli, Italy
[3] supported by EU HCM contract ERB-CHRX-CT93-0376
[4] supported by Worldlab, Lausanne, Switzerland
[5] now a self-employed consultant
[6] now at ELEKLUFT, Bonn
[7] now also at University of Torino
[8] Alexander von Humboldt Fellow
[9] Alfred P. Sloan Foundation Fellow
[10] now at Inst. of Computer Science, Jagellonian Univ., Cracow
[11] now at Comma-Soft, Bonn
[12] visitor from Florida State University
[13] now at Univ. of Mainz
[14] now at DESY Computer Center
[15] supported by European Community Program PRAXIS XXI
[16] now at Dr. Seidel Informationssysteme, Frankfurt/M.
[17] now at Inst. of Accelerating Systems & Applications (IASA), Athens
[18] now at Mercer Management Consulting, Munich
[19] now at Univ. de Strasbourg
[20] now at Andrews University, Barrien Springs, U.S.A.
[21] now with OPAL Collaboration, Faculty of Physics at Univ. of Freiburg
[22] now at SAS-Institut GmbH, Heidelberg
[23] now at GSI Darmstadt
[24] also supported by NSERC
[25] now at Institute for Cosmic Ray Research, University of Tokyo
[26] partially supported by CAM
[27] partially supported by DESY
[28] now at Philips Natlab, Eindhoven, NL
[29] now at Carleton University, Ottawa, Canada
[30] now at Department of Energy, Washington
[31] now at HEP Div., Argonne National Lab., Argonne, IL, USA
[32] now at Oxford Magnet Technology, Eynsham, Oxon
[33] in part supported by Argonne National Laboratory
[34] supported by a MINERVA Fellowship
[35] now at Centre for Subatomic Research, Univ.of Alberta, Canada and TRIUMF, Vancouver, Canada
[36] supported by the Polish State Committee for Scientific Research, grant No. 2P03B09308
[37] supported by the Polish State Committee for Scientific Research, grant No. 2P03B09208
[38] now at University of Colorado, U.S.A.
[39] now at High Energy Group of State University of New York, Stony Brook, N.Y.

[a] supported by the Natural Sciences and Engineering Research Council of Canada (NSERC)
[b] supported by the FCAR of Québec, Canada
[c] supported by the German Federal Ministry for Education and Science, Research and Technology (BMBF), under contract numbers 056BN19I, 056FR19P, 056HH19I, 056HH29I, 056SI79I
[d] supported by the MINERVA Gesellschaft für Forschung GmbH, and by the Israel Academy of Science
[e] supported by the German Israeli Foundation, and by the Israel Academy of Science
[f] supported by the Italian National Institute for Nuclear Physics (INFN)
[g] supported by the Japanese Ministry of Education, Science and Culture (the Monbusho) and its grants for Scientific Research
[h] supported by the Korean Ministry of Education and Korea Science and Engineering Foundation
[i] supported by the Netherlands Foundation for Research on Matter (FOM)
[j] supported by the Polish State Committee for Scientific Research, grants No. 115/E-343/SPUB/P03/109/95, 2P03B 244 08p02, p03, p04 and p05, and the Foundation for Polish-German Collaboration (proj. No. 506/92)
[k] supported by the Polish State Committee for Scientific Research (grant No. 2 P03B 083 08)
[l] partially supported by the German Federal Ministry for Education and Science, Research and Technology (BMBF)
[m] supported by the German Federal Ministry for Education and Science, Research and Technology (BMBF), and the Fund of Fundamental Research of Russian Ministry of Science and Education and by INTAS-Grant No. 93-63
[n] supported by the Spanish Ministry of Education and Science through funds provided by CICYT
[o] supported by the Particle Physics and Astronomy Research Council
[p] supported by the US Department of Energy
[q] supported by the US National Science Foundation

1 Introduction

In high energy hadronic collisions, the dominant mechanism for jet production is described by a hard scatter between partons in the incoming hadrons via a quark or gluon propagator. This propagator carries colour charge. Since colour confinement requires that the final state contain only colour singlet objects, the exchange of colour quantum numbers in the hard process means that a jet at some later stage generally exchanges colour with another jet or beam remnant widely separated from it in rapidity. Such jets are said to be "colour connected" and this leads to the production of particles throughout the rapidity region between the jets. However, if the hard scattering were mediated by the exchange of a colour singlet propagator in the t-channel, each jet would be colour connected only to the beam remnant closest in rapidity and the rapidity region between the jets would contain few final-state particles [1]. The colour singlet propagator could be an electroweak gauge boson or a strongly interacting object, and the soft gluon emission pattern produced in each case is similar [2]. However the rates could be very different. In order to determine the rate of colour singlet exchange processes it has been proposed [3] to study the multiplicity distribution in pseudorapidity[1] (η) and azimuth (φ) of the final state particles in dijet events, and to count events with an absence of particles (i.e. with a rapidity gap) between the two jets.

D0 [4] and CDF [5] have reported the results of searches in $p\bar{p}$ collisions at $\sqrt{s} = 1.8$ TeV for dijet events containing a rapidity gap between the two highest transverse energy (E_T^{jet}) jets. Both collaborations see an excess of gap events over the expectations from colour exchange processes. D0 report an excess of $0.0107 \pm 0.0010(stat.)^{+0.0025}_{-0.0013}(sys.)$, whereas CDF measure the fraction to be 0.0086 ± 0.0012. We report here the results of a similar search in γp interactions obtained from e^+p collisions at HERA.

In leading order, two processes are responsible for jet production in γp interactions at HERA. In the first case, the direct contribution, the photon interacts directly with a parton in the proton. In the second case, the resolved contribution, the photon first fluctuates into a hadronic state which acts as a source of partons which then scatter off partons in the proton. Fig. 1(a) shows schematically an example of colour singlet exchange in resolved photoproduction in which a parton in the photon scatters from a parton in the proton, via t-channel exchange of a colour singlet object. An example of the more common colour non-singlet exchange mechanism is shown in Fig. 1(b). For high E_T^{jet} dijet production, the magnitude of the square of the four-momentum ($|t|$) transferred by the colour singlet object is large. Thus it is possible to calculate in perturbative QCD the cross section for the exchange of a strongly interacting colour singlet object [3, 6, 7, 8]. For instance, the ratio of the two-gluon colour singlet exchange cross section to the single gluon exchange cross section has been estimated to be about 0.1 [3]. Studies of rapidity gaps at high $|t|$ ("hard diffractive scattering") are complementary to studies of diffractive hard scattering where the rapidity gap is between a colourless beam remnant, produced with low four-momentum transfer with respect to one of the beam particles, and hadronic activity in the central detector [9].

The event morphology for the process of Fig. 1(a) is illustrated in Fig. 1(c). There are two jets in the final state, shown as circles in (η, φ) space. Here $\Delta\eta$ is defined as the distance in η

[1] $\eta = -\ln(\tan\frac{\vartheta}{2})$ where ϑ is the polar angle with respect to the z axis, which in the ZEUS coordinate system is defined to be the proton direction.

between the centres of the two jet cones. For the colour singlet exchange process of Fig. 1(a), radiation into the region (labelled "gap") between the jet cones is suppressed, giving rise to the rapidity gap signature. Multiplicity fluctuations in colour non-singlet exchange events can also produce gaps between jets. In order to disentangle the different mechanisms for gap production it is useful to introduce the concept of the 'gap-fraction'.

The gap-fraction, $f(\Delta\eta)$, is defined as the ratio of the number of dijet events at this $\Delta\eta$ which have a rapidity gap between the jets to the total number of dijet events at this $\Delta\eta$. For colour non-singlet exchange, the gap-fraction is expectated to fall exponentially with increasing $\Delta\eta$. This exponential behaviour can be taken as a definition of non-diffractive processes [3]. The expectation follows from the assumption that the probability density for radiation of a particle is constant across the rapidity interval between the jets and it is consistent with the results of analytic QCD calculations [7], and with Monte Carlo simulation (see subsequent sections). For colour singlet exchange, the gap-fraction is not expected to depend strongly upon $\Delta\eta$ [3, 7]. Therefore, at sufficiently large $\Delta\eta$, such a colour singlet contribution will dominate the behaviour of the gap-fraction. The situation is illustrated in Fig. 1 (d), where the colour non-singlet contribution is shown as an exponential fall-off, and the colour singlet contribution is shown as independent of $\Delta\eta$.

In this paper the gap fraction is studied for a sample of photoproduction events with two jets of $E_T^{jet} > 6$ GeV. The events are obtained from an integrated luminosity of 2.6 pb^{-1} of e^+p collisions measured by the ZEUS detector and have γp centre-of-mass energies in the range 135 GeV $< W_{\gamma p} <$ 280 GeV. Dijet cross sections are measured as a function of $\Delta\eta$ for events with a gap and for events with no gap requirement.

2 Experimental Setup

Details of the ZEUS detector have been described elsewhere [10]. The primary components used in this analysis are the central calorimeter and the central tracking detectors. The uranium-scintillator calorimeter [11] covers about 99.7% of the total solid angle and is subdivided into electromagnetic and hadronic sections with respective typical cell sizes, of 5×20 cm^2 (10×20 cm^2 in the rear calorimeter, i.e. the positron direction) and 20×20 cm^2. The central tracking system consists of a vertex detector [12] and a central tracking chamber [13] enclosed in a 1.43 T solenoidal magnetic field.

A photon lead-scintillator calorimeter is used to measure the luminosity via the positron-proton Bremsstrahlung process. This calorimeter is installed inside the HERA tunnel and subtends a small angle in the positron beam direction from the interaction vertex [14]. Low angle scattered positrons are detected in a similar lead-scintillator calorimeter.

In 1994 HERA provided 820 GeV protons and 27.5 GeV positrons colliding in 153 bunches. Additional unpaired positron and proton bunches circulated to allow monitoring of background from beam-gas interactions.

3 Data Selection

The ZEUS data acquisition uses a three level trigger system. At the first level events are selected which were triggered on a coincidence of a regional or transverse energy sum in the calorimeter with a track coming from the interaction region measured in the central tracking chamber. At the second level a cut was made on the total transverse energy, and cuts on calorimeter energies and timing were used to suppress events caused by interactions between the proton beam and residual gas in the beam pipe [15]. At the third level, tracking cuts were made to reject events arising from proton beam-gas interactions and cosmic ray events. Also at the third level, jets were found from the calorimeter cell energies and positions using a fast cone algorithm and events were required to have at least two jets.

Charged current events are rejected by a cut on the missing transverse momentum measured in the calorimeter. Events with a scattered positron candidate in the calorimeter are rejected. This restricts the range of the photon virtuality to $P^2 < 4$ GeV^2, and results in a median P^2 of $\sim 10^{-3}$ GeV^2. A cut of $0.15 \leq y < 0.7$ is applied on the fraction of the positron's momentum which is carried by the photon, where y is reconstructed using the Jacquet-Blondel method [16]. This cut restricts the γp centre-of-mass energies to lie in the range 135 GeV $< W_{\gamma p} <$ 280 GeV.

To select the final jet sample, a cone algorithm [17] is applied to the calorimeter cells. Cells within a radius $R = \sqrt{\delta\eta^2_{cell} + \delta\varphi^2_{cell}}$ of 1.0 from the jet centre are included in the jet where $\delta\eta^{cell}$ amd $\delta\phi^{cell}$ represent respectively the difference in pseudorapidity and azimuthal angle (in radians) between the centre of the cell and the jet axis. Events are then required to have at least two jets found in the uranium calorimeter with $E_T^{jet} > 5$ GeV and $\eta^{jet} < 2.5$. In addition the two highest transverse energy jets[2] were required to have $\Delta\eta > 2$ (i.e. cones not overlapping in η) and boost $|(\eta_1 + \eta_2)|/2 = |\bar{\eta}| < 0.75$. These conditions constrain the jets to lie within the kinematic region where the detector and event simulations are best understood.

To identify gap events, the particle multiplicity is determined by grouping calorimeter cells into "islands". This is done by assigning to every cell a pointer to its highest energy neighbour. A cell which has no highest energy neighbour is a local maximum. An island is formed for each local maximum which includes all of the cells that point to it. The events with *no* islands of transverse energy $E_T^{island} > 250$ MeV and η between the edges of the jet cones (as defined by the cone radius R) are called gap events.

A total of 8393 dijet events were selected, of which 3186 are gap events. The non-e^+p collision background was estimated using the number of events associated with unpaired bunch crossings. The beam gas background was found to be less than 0.1%. The cosmic ray contamination is estimated to be about 0.1%. For those events in which the low angle scattered positron is detected in lead-scintillator calorimeter, $P^2 < 0.02$ GeV^2. The fraction of these events is around 20%, in agreement with the Monte Carlo expectation. The 43 gap events which have $\Delta\eta > 3.5$ were also scanned visually to search for contamination from events where the energy deposits of the scattered positron or a prompt photon might mimic a jet. No such events were found.

[2] In [7] the jets are ordered in pseudorapidity rather than transverse energy and the two jets at lowest and highest pseudorapidity are used in the calculation. When the uncorrected gap-fraction is made with this selection, it is about 0.01 lower.

4 Results

In section 4.1 we present results obtained from ZEUS data which are not corrected for detector effects, by comparing the data to Monte Carlo generated events which have been passed through a detailed simulation of the ZEUS detector and selection criteria. The PYTHIA [18] Monte Carlo program was used with the minimum p_T of the hard scatter set to 2.5 GeV. The GRV [19] parton distributions were used for the photon and the MRSA [20] parton distributions were used for the proton. Two Monte Carlo event samples were generated. For the first sample ("PYTHIA non-singlet"), resolved and direct photon interactions were generated separately and combined according to the cross sections determined by PYTHIA. No electroweak exchange (quark quark scattering via γ/Z^0 or $W^{\pm}$ exchange) events were included. For the second sample ("PYTHIA mixed"), 10% of electroweak exchange events were included. This fraction is two orders of magnitude higher than the level actually expected from the cross section for these events and is chosen in order to mimic the effect of strongly interacting colour singlet exchange processes which are not included in PYTHIA.

In section 4.2 we present the ZEUS data after corrections for all detector acceptance and resolution effects. These hadron-level measurements are then compared to model predictions, and to the expectation of an exponential suppression of gap production for non-diffractive processes.

4.1 Uncorrected Results

The energy flow $1/N dE_T^{cell}/d\delta\eta^{cell}$ with respect to the jet axis for cells within one radian in φ of the jet axis is shown in Fig. 2(a) for the two highest transverse energy jets of each event. PYTHIA mixed events are shown as the solid line. Here and throughout Fig. 2 the data are shown as black dots and the errors shown are statistical only. This jet profile shows highly collimated jets in the data and a pedestal of less than 1 GeV of transverse energy per unit pseudorapidity outside the jet cone radius of 1.0. The pedestal transverse energy is higher toward the proton direction. The superposition of profiles of one jet at high η^{jet} and one at low η^{jet} leads to the bump at $\delta\eta^{cell} \sim 1.5$, due to the forward edge of the calorimeter. The profiles for the PYTHIA non-singlet sample are not shown, as they are similar to those of the mixed sample. The PYTHIA events generally describe the data well, although they are slightly more collimated and underestimate the forward jet pedestal. This small discrepancy may be related to secondary interactions between the photon remnant and the proton remnant, which are not simulated in these PYTHIA samples. Including any kind of multiple interactions in the simulation increases the energy flow and particle multiplicity [21] and thus can only decrease the number of gaps predicted by the Monte Carlo program.

The distribution of the total number of events (without any demand on the presence or absence of a gap) as a function of $\Delta\eta$ is shown in Fig. 2(b). It decreases with increasing $\Delta\eta$, extending out to $\Delta\eta \sim 4$. The PYTHIA distributions are normalized to the number of events in the data. Both PYTHIA samples provide an adequate description of this distribution although the total number of events seen at large $\Delta\eta$ is slightly underestimated.

The distribution of the gap events as a function of $\Delta\eta$ is plotted in Fig. 2(c) where the normalisation for the PYTHIA distribution is the same as in Fig. 2(b). The number of events in the data exhibiting a gap falls steeply with $\Delta\eta$. However the expectation from the PYTHIA non-singlet sample falls more steeply than the data, significantly underestimating the number of gap events at large $\Delta\eta$. The PYTHIA sample with a mixture of 10% of electroweak boson exchange can account for the number of gap events in the data at large $\Delta\eta$. However this sample significantly overestimates the number of gap events at low $\Delta\eta$. As mentioned previously, including secondary interactions in the simulation could reduce the predicted number of gap events and possibly account for this discrepancy.

By taking the ratio of Fig. 2(c) to Fig. 2(b), the gap-fraction shown in Fig. 2(d) is obtained. The gap-fraction falls exponentially out to $\Delta\eta \sim 3.2$. Thereafter it levels off at a value of roughly 0.08. The PYTHIA non-singlet sample fails to describe the flat region in the data, falling approximately exponentially over the whole measured range of $\Delta\eta$. This sample also overestimates the fraction of gap events at low $\Delta\eta$. The PYTHIA mixed sample can describe the flat region of the data but again overestimates the gap-fraction at low $\Delta\eta$. The gap-fraction for the electroweak exchange events alone exceeds 0.4 over the full $\Delta\eta$ range (not shown).

The uncorrected data exhibit a flat region at large $\Delta\eta$ consistent with a colour singlet contribution of around 10%. Detector effects are expected to largely cancel in the gap-fraction. In the next section we find that this is indeed the case and provide quantitative estimates of both the discrepancy between PYTHIA and the data and of the significance of the deviation of the measured gap-fraction from an exponential fall.

4.2 Corrected Results

In order to investigate whether the observed flat region in the gap-fraction might be a detector effect, the PYTHIA mixed sample has been used to correct the data for all detector effects, including acceptance, smearing and the shift in the measurement of energies. Cross sections are determined and the gap-fraction is measured in four bins of $\Delta\eta$ in the range $2 \leq \Delta\eta < 4$.

The cross section $d\sigma/d\Delta\eta$ is measured for dijet photoproduction, $ep \to e\gamma p \to eX$, where X contains at least two jets of final state particles. The cross section is measured in the range $0.2 < y < 0.85$ for photon virtualities $P^2 < 4$ GeV^2. The two jets are defined by a cone algorithm with a cone radius of 1.0 in (η, φ) and satisfy $E_T^{jet} > 6$ GeV, $\eta^{jet} < 2.5$. The two jets of highest E_T^{jet} satisfy $\Delta\eta > 2$ and $|\bar{\eta}| < 0.75$. The rear η^{jet} distribution falls to zero at $\eta^{jet} \sim -2$, well within the rear detector acceptance. Therefore no explicit rear pseudorapidity cut is made. The gap cross section, $d\sigma_{gap}/d\Delta\eta$, is measured, in the same kinematic range, for events with no final state particles with transverse energy $E_T^{particle} > 300$ MeV between the jet cones. The corrected gap-fraction $f(\Delta\eta)$ is then obtained from the ratio of $d\sigma_{gap}/d\Delta\eta$ to $d\sigma/d\Delta\eta$.

The efficiency of the data selection described in section 3 for finding events in this kinematic region was estimated using the Monte Carlo samples. The combined efficiency of the online triggers is at least 80% in every bin of $\Delta\eta$. The efficiency of the offline selection is about 50% leading to a combined efficiency of the online and offline selection criteria of about 40%. The

low efficiency of the offline selection is due to the finite detector resolution of the jet energy and angular variables, and the steeply falling E_T^{jet} spectrum. The shifts and resolutions of these variables are consistent with those obtained in extensive studies of the 1993 dijet sample [22]. The $E_T^{particle}$ resolution is 27% with a shift of -14%. The $\eta^{particle}$ resolution is 0.01 with negligible shift.

The final correction factors for the inclusive cross section are smoothly varying between 1.6 in the lowest $\Delta\eta$ bin and 1.4 in the highest $\Delta\eta$ bin. The correction factors for the gap cross section are between 1.5 and 1.8. The ratios of these correction factors form effective correction factors for the gap-fraction which are all within 27% of unity.

The systematic uncertainties have been estimated by varying the cuts made on the reconstructed quantities. The island algorithm for counting particles was replaced by an algorithm which clusters cells based on proximity in (η, φ) space. Also the results of the bin-by-bin correction were checked using an unfolding procedure [23]. The correction was also performed by using the PYTHIA non-singlet sample and by leaving out the leading order direct contribution. The uncertainty due to the parton distribution was included. The uncertainty due to a 3.3% systematic error in the luminosity measurement was included. Finally the systematic uncertainty arising from a 5% uncertainty in the mean energies measured by the calorimeter was estimated. This represents the largest uncertainty in the two cross sections but cancels in the gap-fraction. The largest systematic uncertainty which remains in the gap-fraction comes from the variation of the E_T^{island} cut from 200 to 300 MeV. The combined effect of these uncertainties is included in the outer error bars in Fig. 3.

The inclusive and gap cross sections and the corrected gap-fraction as a function of $\Delta\eta$ are presented in Figs. 3(a) to (c) respectively (black dots) and compared with the expectations from the PYTHIA non-singlet exchange cross sections (open circles). For the data, the inner error bars show the statistical errors and the outer error bars display the systematic uncertainties, added in quadrature. The cross section points are plotted at the centres of the bins. The gap-fraction points are plotted at the mean $\Delta\eta$ values of the inclusive cross section. Numerical values for the inclusive cross section, the gap cross section and the corrected gap-fraction are provided in Tables 1, 2 and 3, respectively.

The inclusive cross section is around 5 nb per unit $\Delta\eta$ at $\Delta\eta = 2$, falling to about 0.5 nb for $\Delta\eta > 3.5$. The gap cross section is around 3 nb per unit $\Delta\eta$ at $\Delta\eta = 2$ and falls to about 0.06 nb for $\Delta\eta$ between 3.5 and 4. The overall normalization of PYTHIA agrees with the data within the errors. PYTHIA also describes the shape of the inclusive cross section. However it fails to describe the gap cross section, falling too steeply with $\Delta\eta$ and disagreeing significantly in the last bin.

The corrected gap-fraction falls exponentially in the first three bins but the height of the fourth bin is consistent with the height of the third. The height of the fourth bin is $0.11 \pm 0.02(stat.)^{+0.01}_{-0.02}(sys.)$, which is also consistent with the flat region at large $\Delta\eta$ seen in the uncorrected gap fraction and inconsistent with the expectation from PYTHIA.

5 Discussion

Two methods have been used to estimate the significance of the excess of the gap-fraction over the expectation from multiplicity fluctuations in non-singlet exchange.

The first method is to take the difference between the data and the PYTHIA non-singlet gap-fractions, shown in Fig. 3(c). An excess of 0.07 ± 0.03 is obtained, based entirely on the last bin. However this is a model-dependent estimate. For instance replacing the Lund symmetric fragmentation function by the Field-Feynman fragmentation function yields a lower predicted gap-fraction and a larger excess. Introducing multiple interactions into PYTHIA also lowers the fraction of gap events expected. On the other hand, lowering σ_{p_T} (which controls the hadron momentum distribution transverse to the parent parton) in the Monte Carlo simulation from the default value of 0.36 GeV to 0.25 GeV produces a gap-fraction that is very like the data. It has a height in the fourth bin of 0.07 ± 0.02 and therefore if one believes this model, there is no significant excess. However this option yields jet-profiles which are narrower than the default PYTHIA profiles, which are already slightly narrower than the data.

The second way to estimate the excess of the gap-fraction over that expected from purely non-singlet exchange does not rely on comparisons to Monte Carlo predictions. In Fig. 3(d) the gap-fraction is shown again and compared with the result of a two parameter (α,β) χ^2-fit to the expression $f^{fit}(\alpha, \beta; \Delta\eta) = C(\alpha, \beta)e^{\alpha\Delta\eta} + \beta$ where $C(\alpha, \beta)$ is the normalization coefficient constraining $f^{fit}(\alpha, \beta; \Delta\eta)$ to 1.0 at $\Delta\eta = 2$. The result of this fit is shown as the solid curve in Fig 3(d), and the exponential (dotted line) and constant (dashed line) terms are also shown. The quality of this fit, as indicated by the χ^2 value of 1.2 for the two degrees of freedom is superior to that of a fit to an exponential alone which yields $\chi^2 = 9$. The fit parameters are $\alpha = -2.7 \pm 0.3(stat.) \pm 0.1(sys.)$ and $\beta = 0.07 \pm 0.02(stat.)^{+0.01}_{-0.02}(sys.)$. The parameter β gives an estimate of the gap-fraction for colour singlet processes. This method uses the full information of the four measured data points and is not dependent on the details of the Monte Carlo fragmentation model. However, the assumption that the colour singlet gap-fraction is constant with $\Delta\eta$ is only one of many possibilities.

Both the comparison with the default PYTHIA non-singlet prediction and the fit to an exponential form give an excess of about 0.07 in the gap-fraction over the expectation from colour non-singlet exchange.

The excess in the gap-fraction over the expectation from non-singlet exchange may be interpreted as evidence for the exchange of a colour singlet object. In fact the fraction of events due to colour singlet exchange, $\hat{f}(\Delta\eta)$, may be even higher than the measured excess. As previously mentioned, secondary interactions of the photon and proton remnant jets could fill in the gap. A survival probability, $\mathcal{P}$, has been defined [3] which represents the probability that a secondary interaction does not occur. Then $f(\Delta\eta) = \hat{f}(\Delta\eta) \cdot \mathcal{P}$. Estimates of the survival probability for $p\bar{p}$ collisions at the Tevatron range from about 5% to 30% [3, 24, 25]. The survival probability at HERA could be higher due to the lower centre-of-mass energy, the fact that one remnant jet comes from a photon rather than a proton and the fact that the mean fraction of the photon energy participating in the jet production in these events is high[3]. Therefore the ZEUS result

[3]The average fraction of the photon energy participating in the production of the two jets [22] is 0.7 for these events. Nevertheless, according to the PYTHIA simulation the dominant contribution in this kinematic regime is from leading order resolved events.

of ~ 0.07 and the D0 and CDF results of $0.0107 \pm 0.0010(stat.)^{+0.0025}_{-0.0013}(sys.)$ and 0.0086 ± 0.0012 could arise from the same underlying process.

The magnitude of the squared four-momentum transfer across the rapidity gap as calculated from the jets is large ($|t| \geq (E_T^{jet})^2$). Thus the colour singlet exchange is unambiguously "hard".

The PYTHIA generator predicts that the ratio of the electroweak (σ^{EW}) to QCD (σ^{QCD}) exchange cross sections in this kinematic range is $\sigma^{EW}/\sigma^{QCD} < 7 \cdot 10^{-4}$ (compatible with the estimation $(\alpha/\alpha_s)^2$). Therefore quark quark scattering via γ/Z^0 and $W^{\pm}$ exchange cannot explain the height of the flat region in the gap-fraction. On the other hand, using the simple two-gluon model for pomeron exchange gives $\hat{f}(\Delta\eta) \sim 0.1$ [3]. Thus pomeron exchange could account for the data.

In summary, dijet photoproduction events with $E_T^{jet} > 6$ GeV contain an excess of events with a rapidity gap between the two jets over the expectations of colour exchange processes. This excess is observed as a flat region in the gap-fraction at large rapidity separation ($\Delta\eta = 3.7$) at a level of $0.11 \pm 0.02(stat.)^{+0.01}_{-0.02}(sys.)$. It can be interpreted as evidence of hard diffractive scattering via a strongly interacting colour singlet object.

Acknowledgements

We thank the DESY Directorate for their strong support and encouragement and the HERA machine group for providing colliding beams. We acknowledge the assistance of the DESY computing and networking staff. It is also a pleasure to thank V. Del Duca for useful discussions.

References

[1] Y. Dokshitzer, V. Khoze and S. Troyan, in Proceedings of the 6th International Conference on Physics in Collisions, Chicago, Illinois, ed. M. Derrick (World Scientific, Singapore, 1987) 417.

[2] H. N. Chehime and D. Zeppenfeld, MAD/PH/814 (1994).

[3] J. D. Bjorken, Phys. Rev. D47 (1992) 101.

[4] D0 Collaboration, S. Abachi et al., Phys. Rev. Lett. 72 (1994) 2332;
D0 Collaboration, S. Abachi et al., FERMILAB-PUB-95-302-E (1995).

[5] CDF Collaboration, F. Abe, et al., Phys. Rev. Lett. 74 (1995) 855.

[6] A. H. Mueller and W.-K. Tang, Phys. Lett. B284 (1992) 123.

[7] V. Del Duca and W.-K. Tang, Phys. Lett. B312 (1993) 225.

[8] H. J. Lu, AZPH-TH/95-21 (1995).

[9] UA8 Collaboration, A. Brandt et al., Phys. Lett. B211 (1988) 239, B297 (1992) 417;
ZEUS Collaboration, M. Derrick et al., Phys. Lett. B315 (1993) 481 ; DESY 95-093 (1995); Phys. Lett. B356 (1995) 129 and references therein ;
H1 Collaboration, I. Abt et al., Nucl. Phys. B429 (1994) 477 ; Phys. Lett. B348 (1995) 681.

[10] ZEUS Collaboration, The ZEUS detector, Status Report (1993)

[11] M. Derrick et al., Nuc. Instr. and Meth. A309 (1991) 77;
A. Andresen et al., Nuc. Instr. and Meth. A309 (1991) 101;
A. Bernstein et al., Nuc. Instr. and Meth. A336 (1993) 23.

[12] C. Alvisi et al., Nuc. Instr. and Meth. A305 (1991) 30.

[13] B. Foster et al., Nucl. Phys. B, Proc. Suppl. B32 (1993) 181.

[14] J. Andruszków et al., DESY 92-066 (1992).

[15] ZEUS Collaboration, M. Derrick et al., Phys. Lett. B316 (1993) 412.

[16] F. Jacquet and A. Blondel, in Proceedings of the study of an *ep* facility for Europe, Hamburg, ed. U. Amaldi, (DESY 79/48, 1979) 391.

[17] J. Huth et al., in Proceedings of the 1990 DPF Summer Study on High Energy Physics, Snowmass, Colorado, ed. E.L. Berger (World Scientific, Singapore, 1992) 134;
UA1 Collaboration, G. Arnison et al., Phys. Lett. 123B (1983) 115.

[18] H.-U. Bengtsson and T. Sjöstrand, Comp. Phys. Comm. 46 (1987) 43;
T. Sjöstrand, CERN-TH.6488/92 (1992).

[19] M. Glück, E. Reya and A. Vogt, Phys. Rev. D46 (1992) 1973.

[20] A. Martin, W.J. Stirling and R.G. Roberts, Phys. Rev. D50 (1994) 6734.

[21] T. Sjöstrand and M. van Zijl, Phys. Rev. D36 (1987) 2019;
G. A. Schuler and T. Sjöstrand, Phys. Lett. B300 (1993) 169; Nucl. Phys. B407 (1993) 539;
J. M. Butterworth and J. R. Forshaw, J. Phys. G19 (1993) 1657;
J. M. Butterworth et al, CERN-TH-95-83 (1995).

[22] ZEUS Collaboration, M. Derrick et al., Phys. Lett. B348 (1995) 665.

[23] G. D'Agostini, Nucl. Instr. Meth. A367 (1995) 487.

[24] E. Gotsman, E. M. Levin and U. Maor, Phys. Lett. B309 (1993) 199.

[25] R. S. Fletcher and T. Stelzer, Phys. Rev. D48 (1993) 5162.

$\Delta\eta$	$d\sigma/d\Delta\eta$ (nb)	Statistical Uncertainty (nb)	Systematic Uncertainty (nb)
2.25	4.93	0.24	$^{+0.83}_{-0.68}$
2.75	3.06	0.15	$^{+0.54}_{-0.52}$
3.25	1.67	0.07	$^{+0.31}_{-0.19}$
3.75	0.54	0.03	$^{+0.08}_{-0.03}$

Table 1: $d\sigma/d\Delta\eta$ for $ep \to e\gamma p \to eX$ in the kinematic range $0.2 < y < 0.8$ and $P^2 < 4$ GeV^2 and where X contains two or more jets of $E_T^{jet} > 6$ GeV, $\eta^{jet} < 2.5$, $|\bar{\eta}| < 0.75$ and $\Delta\eta > 2$.

$\Delta\eta$	$d\sigma^{gap}/d\Delta\eta$ (nb)	Statistical Uncertainty (nb)	Systematic Uncertainty (nb)
2.25	2.85	0.17	$^{+0.45}_{-0.45}$
2.75	0.66	0.06	$^{+0.11}_{-0.15}$
3.25	0.16	0.02	$^{+0.03}_{-0.04}$
3.75	0.06	0.01	$^{+0.01}_{-0.01}$

Table 2: $d\sigma^{gap}/d\Delta\eta$ for $ep \to e\gamma p \to eX$ in the kinematic range $0.2 < y < 0.8$ and $P^2 < 4$ GeV^2 and where X contains two or more jets of $E_T^{jet} > 6$ GeV, $\eta^{jet} < 2.5$, $|\bar{\eta}| < 0.75$ and $\Delta\eta > 2$ with *no* final state particles of $E_T^{particle} > 300$ MeV between the jets.

$\Delta\eta$	$f(\Delta\eta)$	Statistical Uncertainty	Systematic Uncertainty
2.23	0.58	0.04	$^{+0.04}_{-0.02}$
2.73	0.22	0.02	$^{+0.02}_{-0.02}$
3.22	0.10	0.01	$^{+0.01}_{-0.02}$
3.70	0.11	0.02	$^{+0.01}_{-0.02}$

Table 3: The gap-fraction, $f(\Delta\eta)$, for $ep \to e\gamma p \to eX$ in the kinematic range $0.2 < y < 0.8$ and $P^2 < 4$ GeV^2 and where X contains two or more jets of $E_T^{jet} > 6$ GeV, $\eta^{jet} < 2.5$, $|\bar{\eta}| < 0.75$ and $\Delta\eta > 2$.

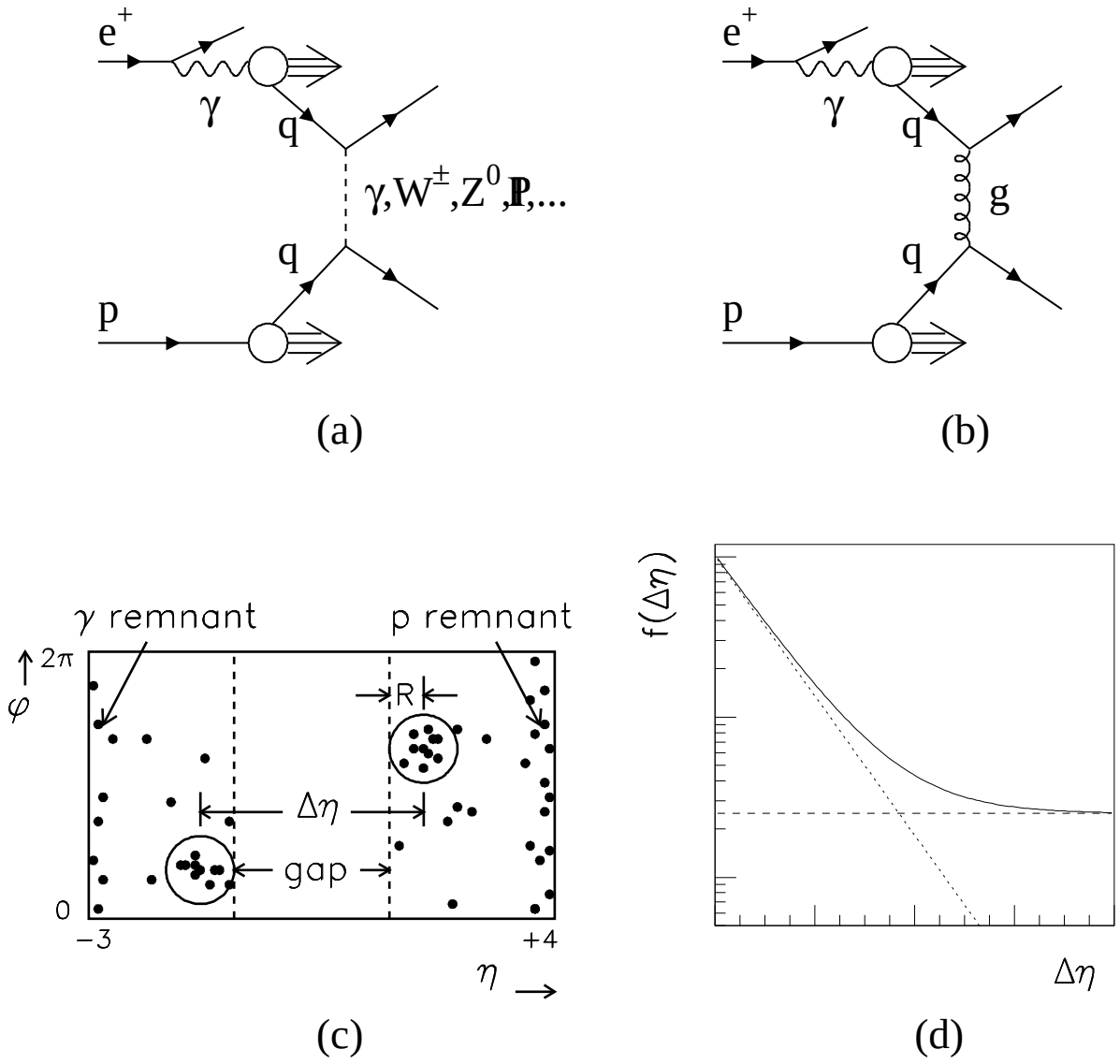

Figure 1: Resolved photoproduction via (a) colour singlet exchange and (b) colour non-singlet exchange. The rapidity gap event morphology is shown in (c) where black dots represent final state hadrons and the boundary illustrates the limit of the ZEUS acceptance. Two jets of radius R are shown, which are back to back in azimuth and separated by a pseudorapidity interval $\Delta\eta$. An expectation for the behaviour of the gap fraction is shown in (d)(solid line). The non-singlet contribution is shown as the dotted line and the colour singlet contribution as the dashed line.

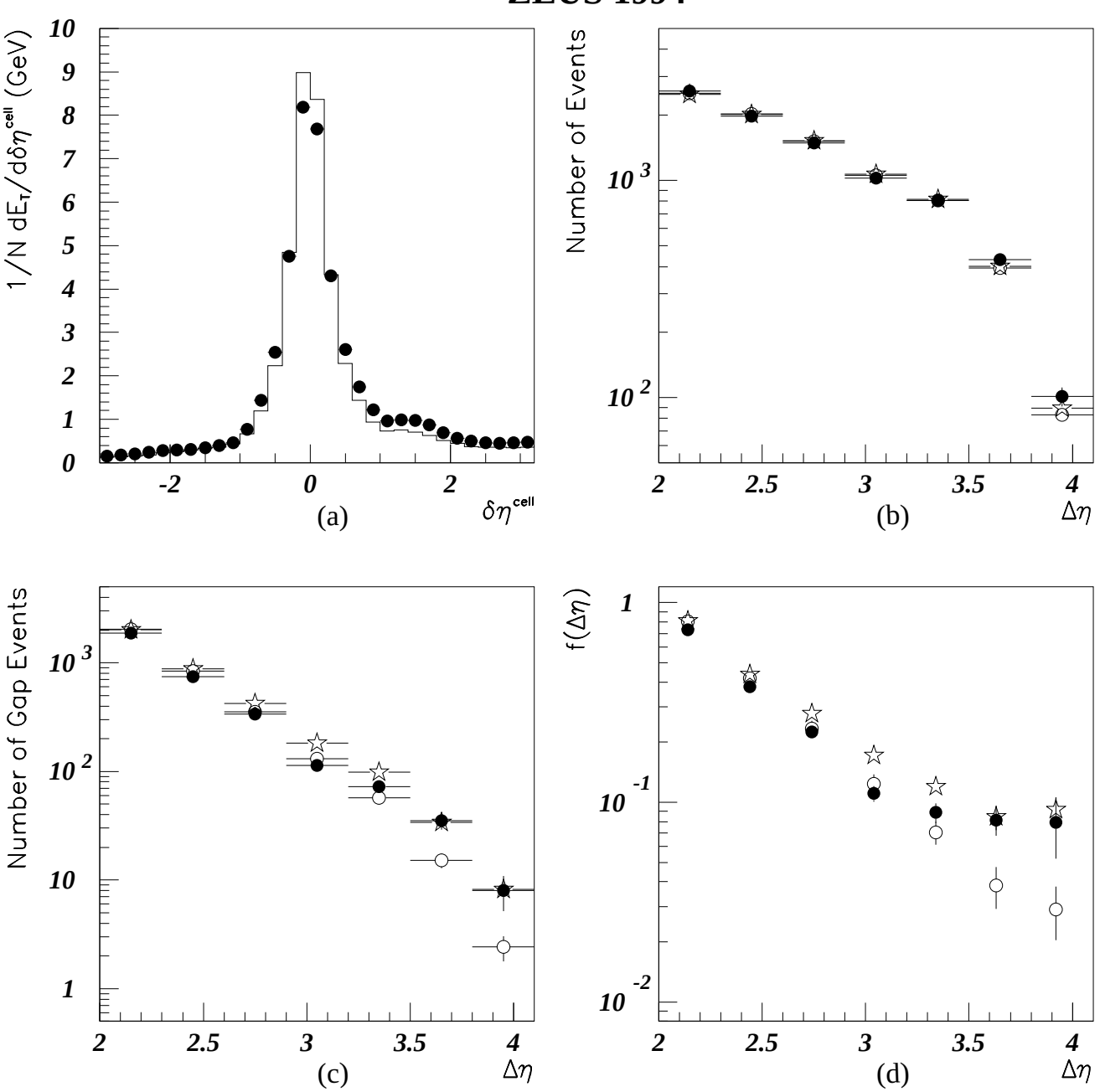

Figure 2: Uncorrected data compared with the predictions from PYTHIA events which have been passed through a detailed simulation of the ZEUS detector and of the sample selection criteria. The errors shown are statistical only. The transverse energy flow with respect to the jet axis is shown in (a) where the data are shown as black dots and the PYTHIA non-singlet sample is shown as a solid line. In (b), (c) and (d) the data are again shown as black dots. The PYTHIA non-singlet sample is shown as open circles and the PYTHIA mixed sample (which contains 10% of colour singlet exchange events) is shown as stars. The number of events versus $\Delta\eta$ is shown in (b). The number of gap events versus $\Delta\eta$ is shown in (c) and the gap-fraction is shown in (d). In (d) the points are drawn at the mean $\Delta\eta$ of the inclusive distribution in the corresponding bin.

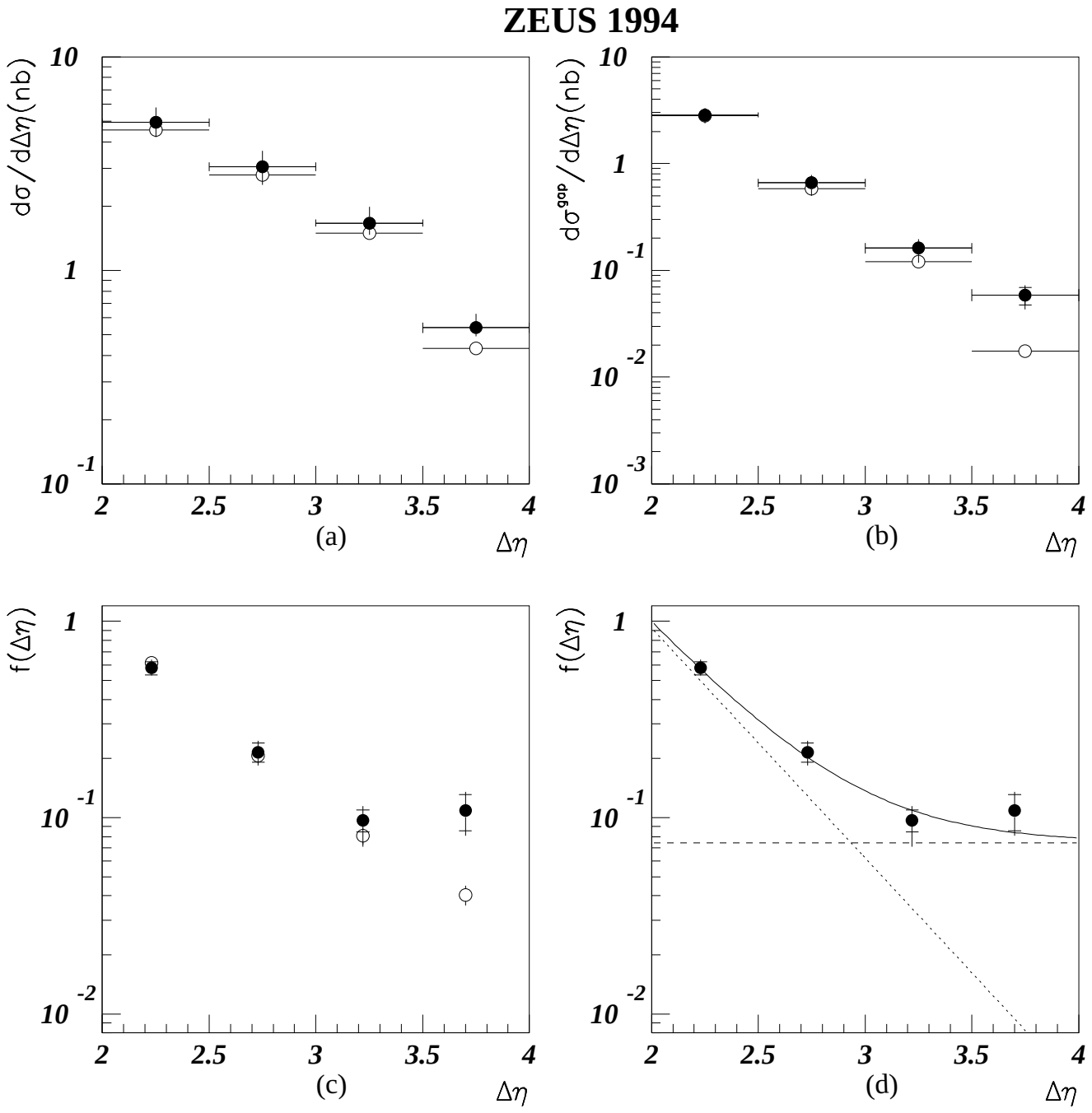

Figure 3: ZEUS data (black circles) corrected for detector effects. The inner error bars represent the statistical errors from the data and Monte Carlo samples, and the outer error bars include the systematic uncertainty, added in quadrature. In (a), (b) and (c) the PYTHIA prediction for non-singlet exchange events is shown as open circles. The inclusive cross section is shown in (a). The cross section for gap events is shown in (b) and the gap-fraction is shown in (c). The gap-fraction is redisplayed in (d) and compared with the result of a fit to an exponential plus a constant. In (c) and (d) the points are drawn at the mean $\Delta\eta$ of the inclusive distribution in the corresponding bin.